# Dependence of local electronic structure in *p*-type GaN on crystal polarity and presence of inversion domain boundaries

X. Zhou and E. T. Yu[a)]
*Department of Electrical and Computer Engineering, University of California, San Diego, La Jolla, California 92093-0407*

D. S. Green and J. S. Speck
*Materials Department, University of California, Santa Barbara, Santa Barbara, California 93106*

(Received 10 June 2005; accepted 5 December 2005; published 19 January 2006)

Scanning probe techniques including scanning capacitance microscopy, scanning capacitance spectroscopy, scanning Kelvin probe force microscopy, and atomic force microscopy have been used to assess structure and local electronic properties of Ga-face and N-face *p*-type GaN and of inversion domain boundaries in *p*-type GaN. Epitaxial layers of *p*-type GaN were grown by molecular-beam epitaxy, and by adjustment of the Ga:N flux ratio samples containing both Ga-face and N-face material were obtained. Under identical growth conditions, net incorporation of electrically active Mg acceptors was found to be more efficient for material with Ga-face polarity. Only a very small dependence of surface potential on polarity was observed, in contrast to results reported for *n*-type GaN, in which a substantial dependence of Schottky barrier height on polarity has been found. In addition, elevated net concentrations of ionized Mg acceptors were observed in Ga-face regions in the immediate vicinity of some, but not all, inversion domain boundaries, consistent with theoretical suggestions that incorporation of high concentrations of Mg within an inversion domain boundary can lead to increased concentrations of Mg acceptors near the inversion domain boundary.  [DOI: 10.1116/1.2162577]

## I. INTRODUCTION

Efficient acceptor doping of group-III nitride semiconductors is an essential requirement for a wide range of nitride-based electronic and optoelectronic devices including heterojunction bipolar transistors, visible light-emitting diodes, and lasers. Unfortunately, *p*-type doping of GaN has proven to be highly challenging, as the most widely used dopant species, Mg, suffers from a very high ionization energy, resulting in a room-temperature free hole concentration that is much lower than the total acceptor concentration. Furthermore, hole concentrations in *p*-type GaN are typically observed to saturate and decrease at high Mg concentrations,[1,2] and high levels of Mg incorporation are found to lead to increased defect formation,[3,4] with the presence of defects such as dislocations influencing the spatial distribution of Mg acceptors.[5] Finally, the crystal polarity during growth of GaN by molecular-beam epitaxy (MBE) has been observed to invert from Ga face to N face upon exposure to Mg;[6] the observed polarity inversion has been found to be dependent on the Ga:N flux ratio, with decreased Ga flux leading to inversion of polarity from Ga face to N face.[7]

Given the difficulties associated with efficient acceptor doping of GaN, an understanding of the relationships among active acceptor concentration, the existence and spatial distribution of defects, crystal polarity, and other factors is critical. In this article we describe spatially resolved studies of local electronic structure in *p*-type GaN as a function of crystal polarity and in the vicinity of inversion domain boundaries. Scanning capacitance microscopy (SCM) and spectroscopy were used to image, on a local basis, surface potential and net ionized acceptor distributions in *p*-type GaN films grown by MBE. Because the *p*-type GaN films were grown under conditions leading to the presence of both Ga-polar and N-polar materials, a direct assessment of net Mg acceptor incorporation under identical growth conditions and its dependence on crystal polarity is possible. In addition, possible variations in net Mg acceptor incorporation in the vicinity of inversion domain boundaries, which have been proposed to contain increased concentrations of Mg in *p*-type GaN,[8,9] can be detected. Our results indicate that net Mg acceptor incorporation varies significantly with crystal polarity, being more efficient for Ga-polar than for N-polar material. Furthermore, we observe evidence that in some, but not all, instances increased net concentrations of ionized Mg acceptors can be present within or near inversion domain boundaries and other bulk defects.

## II. EXPERIMENT

The epitaxial layer structures employed in these studies consisted of 0.4-$\mu$m-thick *p*-type GaN layers grown by MBE on $\sim$2 $\mu$m GaN templates grown by metal-organic chemical-vapor deposition (MOCVD) on sapphire substrates. Details of the growth conditions employed are described elsewhere.[10] In brief, the samples were grown in a Varian Modular Gen II system using conventional effusion cells for Mg and Ga. Active nitrogen was supplied by an EPI Unibulb rf plasma source. All samples were grown with a rf power of 150 W, a substrate temperature of 650 °C, and a

a)Electronic mail: ety@ece.ucsd.edu

sufficient $N_2$ flow to maintain chamber pressure of $1.1 \times 10^{-5}$ Torr. These conditions yielded a nominal growth rate of 200 nm/h for Ga-rich growth. Prior studies have shown that exposure of GaN to Mg during MBE growth can lead to inversion of crystal polarity from Ga face to N face and that the extent of inversion depends on the Ga:N flux ratio. Specifically, the presence of a Ga wetting layer on the surface during growth is found to lead to Ga-face polarity, while the absence of such a wetting layer results in N-face growth.[7] By adjusting the Ga:N flux ratio during MBE growth, the presence and spatial distribution of a Ga wetting layer on the surface can be controlled, and hence fully Ga-face growth, fully N-face growth, or an intermediate situation with regions of each polarity can be achieved. For these studies, three samples were employed, grown with Ga fluxes of $3.3 \times 10^{-7}$, $3.1 \times 10^{-7}$, and $2.9 \times 10^{-7}$ Torr. The first two samples were found on the basis of postgrowth reflection high-energy electron diffraction (RHEED) and atomic force microscopy (AFM) to contain exclusively Ga-polar material while the last contained regions of both Ga-face and N-face materials. The results shown in Sec. III were obtained exclusively on the sample with mixed polarity.

Samples were stored under ambient atmospheric conditions and cleaned with trichloroethylene, acetone, and isopropanol in an ultrasonic bath prior to scanning probe characterization. Ohmic contacts to the top *p*-type GaN surface were fabricated by deposition of Ni/Au metallization and subsequent rapid thermal annealing in $H_2/N_2$ at 500 °C for 30 s. AFM, SCM, scanning capacitance spectroscopy (SCS), and scanning Kelvin probe force microscopy (SKPM) measurements were performed in a Digital Instruments/Veeco Nanoscope IIIa Dimension 3100 system under ambient atmospheric conditions—typically ~20 °C with ~50% relative humidity. Co/Cr-coated probe tips with a nominal radius of 25 nm at the tip apex were used for the AFM, SCM, SCS, and SKPM studies. Crystal polarities for each sample and within individual samples were determined by wet chemical etching in 160 °C $H_3PO_4$, which has been shown to etch N-polar material while leaving Ga-polar material unaffected,[11,12] followed by evaluation of surface morphology and etch depth using AFM.

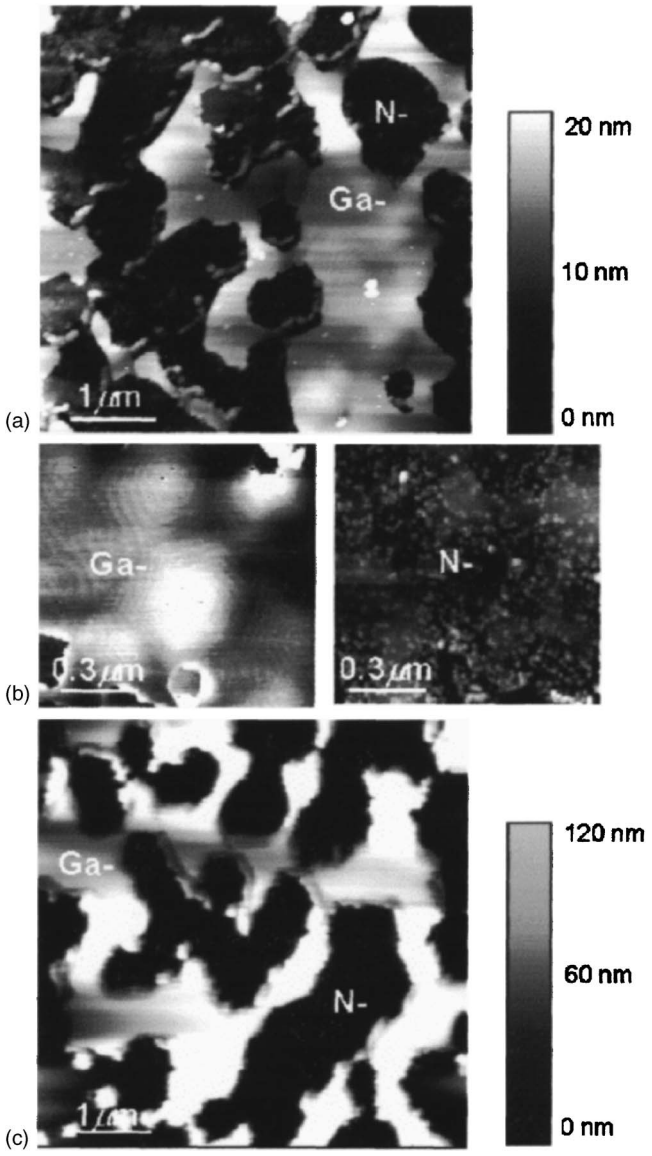


FIG. 1. (a) $5 \times 5$ $\mu m^2$ AFM image of as-grown Mg-doped *p*-type GaN and (b) magnified view of Ga-face (left) and N-face (right) surface topographies. (c) AFM surface topography after exposure to hot $H_3PO_4$, which etches N-face GaN while leaving material with Ga-face polarity unchanged. Areas identified as possessing N-face and Ga-face polarities on this basis are indicated.

## III. RESULTS AND DISCUSSION

AFM imaging combined with etching in hot $H_3PO_4$ of the mixed-polarity sample confirmed the presence of both Ga-face and N-face regions and enabled correlation of preetch surface topography with local crystal polarity. Figures 1(a) and 1(b) show AFM images of the initial surface topography for this sample, with regions identified as Ga-face and N-face polarities indicated. The polarity distribution in the sample was not uniform, i.e., some regions contained primarily Ga-face material with N-face inversion domains, while other regions contained predominantly N-face material. Terraces separated by atomic steps as well as spiral growth hillocks are typically visible in the Ga-face regions. Regions identified as N-face polarity were initially about 20 nm lower topographically than the surrounding Ga-face material and exhibited rougher surface topography including high densities of growth hillocks approximately 3–5 nm in height. Figure 1(c) shows an AFM topograph of the same sample following etching in hot $H_3PO_4$. The surface morphology in the Ga-face regions is essentially unchanged while that in the N-face regions exhibits increased roughness with the surface being much lower topographically, relative to the Ga-face regions, than prior to etching. The measured rms for local Ga-face and N-face regions are 2.1 and 6.2 nm, respectively. The etch rate for the N-face region was estimated to be ~200 nm/min. These observations provided confirmation for the assignment of Ga-face or N-face polarity to different regions of the sample.

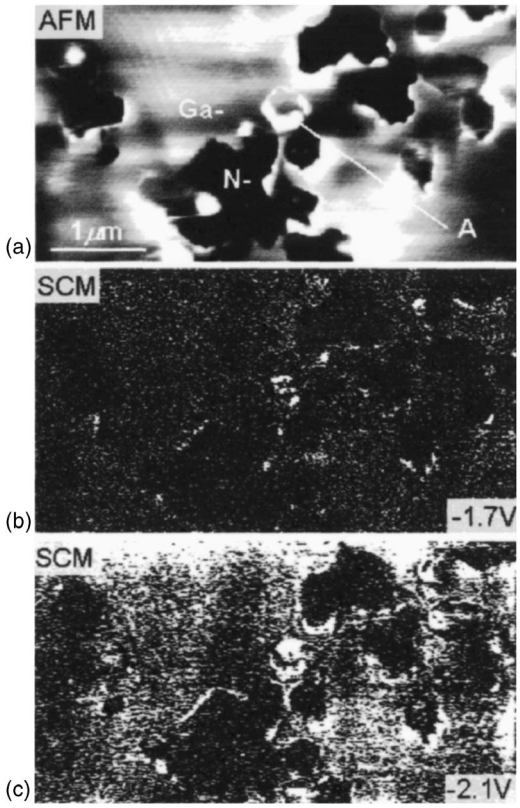


FIG. 2. (a) AFM topograph and [(b) and (c)] SCM images of the same region with dc bias voltages applied to the tip of −1.7 and −2.1 V. Over this range of bias voltages, a larger SCM signal is observed within Ga-face regions than in N-face regions. In the immediate vicinity of some, but not all, inversion domain boundaries, a further increase in SCM signal level is observed.

SCM images were acquired as a function of bias voltage applied between the probe tip and sample for dc bias voltages ranging from 0 to −2.5 V, with an additional ac bias voltage modulation of 1 V in amplitude applied at a frequency of 30 kHz. Figure 2 shows a $2.5\times5$ $\mu m^2$ AFM topograph of the *p*-type GaN surface and SCM images of the same area obtained with tip bias voltages of −1.7 and −2.1 V. Ga-face and N-face regions are identified on the basis of surface morphology and topographic height, as indicated in the figure. In addition, hexagonal features surrounded by perimeter regions of elevated topography, such as that marked "A" in Fig. 2(a), are occasionally visible in the AFM image; on the basis of the aforementioned etching studies we conclude that these hexagonal features contain Ga-face material.

The SCM images shown in Fig. 2 reveal local variations in SCM signal level that are correlated with the local crystal polarity or, in some cases, the presence of an inversion domain boundary. For tip bias voltages ranging from 0 to −1.5 V, SCM images of the *p*-GaN surface (not shown) reveal negligible signal contrast. For tip bias voltages of −1.7 V and below, contrast develops in which a higher signal level is observed in regions of Ga-face polarity than in regions of N-face polarity. This is evident in Figs. 2(b) and 2(c), in which lower SCM signal levels (dark) are observed in regions identified as N-polar on the basis of surface topography as shown in Fig. 2(a). The difference in SCM signal level observed in Ga-polar versus N-polar regions increases as the tip bias voltage becomes more negative. In addition, a high SCM signal level—higher even than that observed in Ga-face regions—is observed in the immediate vicinity of some, but not all, inversion domain boundaries. This behavior becomes more pronounced as the tip bias voltage becomes more negative and is most evident in Fig. 2(c).

The relationship between SCM signal level and net ionized Mg acceptor concentration in our studies can be understood as follows. In the SCM measurement, the tip-sample junction is incorporated into an *RLC* circuit whose resonant frequency depends on the tip-sample capacitance. The circuit is driven near its resonant frequency, and the resulting output signal obtained in the scanning capacitance measurement is proportional to the derivative of the tip-sample capacitance with respect to voltage.[13,14] Because any oxide or contamination layers present on the tip or sample surfaces during these measurements are expected to be very thin in comparison to the depth of the depletion region extending into the semiconductor, the tip-sample capacitance can be approximated as that of a Schottky contact. In a one-dimensional approximation, the tip-sample capacitance per unit area $C$ is then given by[15]

$$C = \varepsilon_s / W, \tag{1}$$

$$W = \sqrt{\frac{2\varepsilon_s}{qN_A}\left(\phi_b - \frac{k_B T}{q}\ln\frac{N_v}{N_A} + V + \frac{k_B T}{q}\right)}, \tag{2}$$

where $\varepsilon_s$ is the semiconductor dielectric constant, $W$ is the semiconductor depletion depth, $N_A$ is the net ionized acceptor concentration, $\phi_b$ is the *p*-type Schottky barrier height, $N_v$ is the valence-band effective density of states, $V$ is the dc component of the tip bias relative to the sample, $T$ is the temperature, $k_B$ is Boltzmann's constant, and $q$ is the electron charge. The SCM signal is then proportional to $|dC/dV|$, which from Eqs. (1) and (2) is given by

$$\left|\frac{dC}{dV}\right| = \frac{1}{2}\sqrt{\frac{q\varepsilon_s N_A}{2}}\left(\phi_b - \frac{k_B T}{q}\ln\frac{N_v}{N_A} + V + \frac{k_B T}{q}\right)^{-3/2}. \tag{3}$$

From Eq. (3) we see that local variations in the SCM signal will arise primarily from inhomogeneity in net ionized acceptor concentration $N_A$ or local surface barrier height $\phi_b$. Variations in local surface barrier height can be probed by SKPM,[16,17] in which the contact potential difference between a conducting probe tip and the sample surface is imaged. Figure 3 shows an AFM topograph, an SKPM image, obtained simultaneously, of the *p*-GaN surface, along with a plot of local surface potential extracted from the SKPM image. Regions of both Ga-face and N-face polarities are present in the images, with the N-face regions exhibiting a surface potential ~0.02–0.06 V higher than that of the Ga-face regions. This is in contrast to observations reported for *n*-type GaN, for which differences in Schottky barrier height of 0.2–0.5 V were observed in comparisons of Schottky contacts to Ga-face and N-face *n*-type GaN.[18,19] Since the

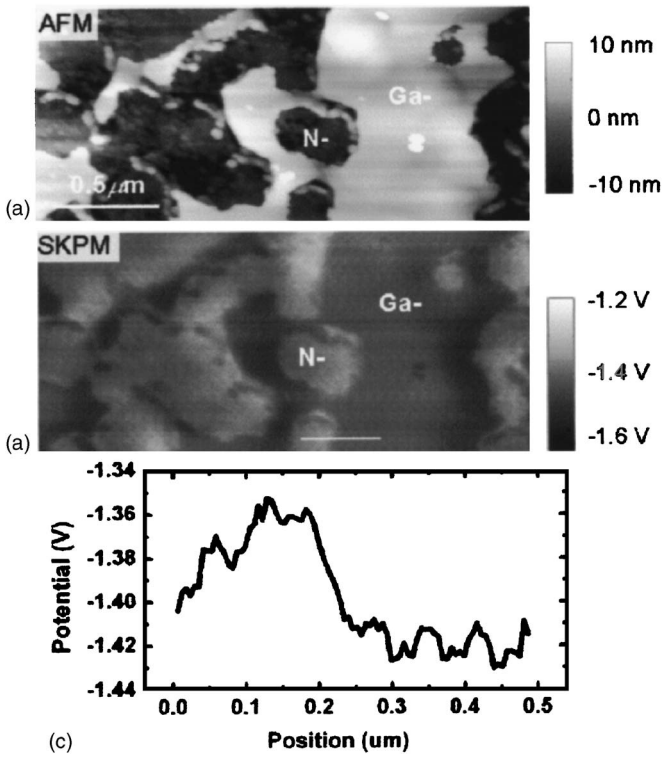


FIG. 3. (a) AFM topograph and (b) SKPM image, obtained simultaneously, of Ga-face and N-face regions of the *p*-type GaN surface. Comparison of Ga-face and N-face regions indicates that the N-face region has a contact potential approximately 0.02 V higher than that of the Ga-face region. (c) Surface-potential profile, measured relative to the surface potential of the probe tip, extracted from SKPM image data along the line shown in (b).

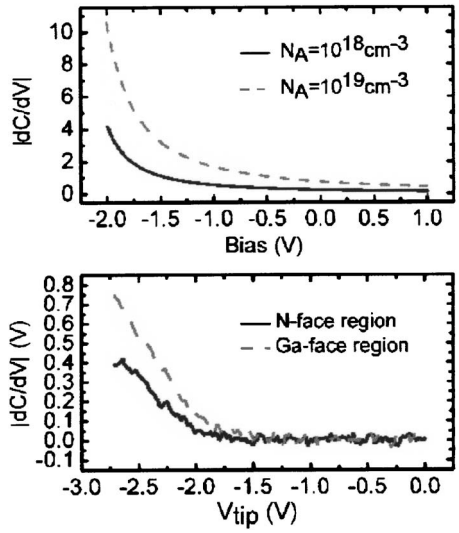


FIG. 4. (a) Computed $|dC/dV|$ as a function of $V$ for *p*-type GaN with net ionized Mg acceptor concentrations of $1\times10^{18}$ cm$^{-3}$ (solid line) and $1\times10^{19}$ cm$^{-3}$ (dashed line). (b) Scanning capacitance spectra obtained for N-face (solid line) and Ga-face (dashed line) areas of the sample surface.

observed difference in surface potential for Ga face compared to N-face *p*-type GaN is much smaller than the expected surface barrier height $\phi_b$, the accompanying difference in SCM signal level between Ga-face and N-face regions arising from the variation in surface barrier height will be negligible. Thus, the principal source of the signal contrast observed in our SCM imaging is expected to be local variations in net ionized Mg acceptor concentration.

Figure 4(a) shows a plot of $|dC/dV|$ computed as a function of $V$ for net ionized Mg acceptor concentrations of $1\times10^{18}$ cm$^{-3}$ (solid line) and $1\times10^{19}$ cm$^{-3}$ (dashed line). It is evident from the figure that for sufficiently negative tip bias voltages, regions of the sample with higher net ionized Mg acceptor concentration will be characterized by a larger value of $|dC/dV|$ and hence a larger SCM signal level, than regions with lower net ionized Mg concentration. Thus, we interpret the higher SCM signal levels observed in regions of Ga-face polarity relative to those in N-face regions as arising from a higher degree of net Mg acceptor incorporation for material with Ga-face polarity compared to that for N-face material.

We refer throughout to the net rather than the total acceptor concentrations to allow for the possibility of decreased compensation by donorlike states, rather than solely increased Mg acceptor incorporation, as a source of localized increases in SCM signal level observed in various regions of the sample. However, it is expected that the possible presence of such donorlike states is unlikely to exert a strong influence on the observed SCM signal levels. Because the SCM imaging and analysis presented here are for forward-bias conditions, donorlike trap states near the conduction-band edge will not cross the Fermi level during our measurements, and emission rates for donorlike states that do cross the Fermi level under forward-bias voltages are likely to be very low compared to the measurement frequency due to the large activation energies for electron emission that would characterize such levels.

Our interpretation of the SCM imaging data is further confirmed by SCS measurements. The scanning capacitance spectra were obtained in the "magnitude mode" of operation of the scanning capacitance instrument, and the signal plotted is therefore proportional to $|dC/dV|$, where $C$ is the tip-sample capacitance. Figure 4(b) shows scanning capacitance signal spectra acquired on regions of Ga-face (dashed line) and N-face (solid line) polarities. A comparison of these measured spectra with those computed and shown in Fig. 4(a) indicates quite clearly that net ionized Mg acceptor concentration variations are the principal source of SCM signal contrast between Ga-face and N-face regions of the sample. The apparent shift in bias voltage between the calculated and measured capacitance spectra is due principally to contact and series resistance effects, as confirmed by local measurements of current-voltage spectra by conductive AFM, and to the effects of finite tip size and tip shape.[20] Thus, these results demonstrate that under identical growth conditions, net Mg acceptor incorporation is more efficient for Ga-face compared to N-face material. This observation is consistent with prior reports that Mg doping of GaN results in greater total Mg incorporation[8] and higher *p*-type conductivity[21] for material grown with Ga-face polarity compared to N-face material and suggests that avoidance of inversion domain formation is essential for optimization of *p*-type conductivity in GaN.

In addition to revealing higher net Mg acceptor incorporation into Ga-face compared to N-face material, SCM imaging indicates that higher net concentrations of ionized Mg acceptors can occasionally be present in the immediate vicinity of inversion domain boundaries than in the surrounding Ga-face and N-face materials. Examination of the SCM images in Fig. 2 reveals that in certain areas, the boundaries between Ga-face and N-face materials exhibit a higher SCM signal level than observed in the surrounding regions, indicating that an increased net ionized Mg acceptor concentration is present within or in the immediate vicinity of the inversion domain boundaries. These regions of increased net ionized Mg acceptor concentration typically extend approximately 30–50 nm away from the inversion domain boundary. That these SCM contrast features are not observed at all inversion domain boundaries and that they are not observed in the vicinity of other topographic features of similar size and abruptness indicate that these features represent true variations in local electronic properties rather than being simply topography-induced imaging artifacts. The areas of increased net ionized Mg acceptor concentration near inversion domain boundaries appear to extend preferentially into adjacent Ga-face regions, suggesting the possibility of segregation of Mg to inversion domain boundaries from adjacent Ga-face regions. Such an occurrence would not be entirely unexpected, as theoretical studies have suggested that increased Mg acceptor concentrations may be favored in the vicinity of inversion domain boundaries containing high concentrations of Mg.[9] The results presented here show directly that elevated net concentrations of ionized Mg acceptors can be present near inversion domain boundaries, suggesting that substantial concentrations of Mg may be present within the inversion domain boundary itself.

Finally, we note that the hexagonal features observed in regions of Ga-face polarity exhibit higher SCM signal levels, which are indicative of increased net concentrations of ionized Mg acceptors, than do the surrounding Ga-face regions. However, the topographically elevated areas on the perimeter of these hexagonal regions exhibit a lower net concentration of ionized Mg acceptors near the interior perimeter boundary and higher net ionized Mg acceptor concentrations exterior to the hexagonal regions. Those observations suggest that either segregation of active Mg acceptors from the hexagon perimeter or else reduced incorporation or increased compensation of Mg acceptors near the perimeter occurs in these regions. However, the specific nature and mechanism for formation of such defects is not known.

## IV. CONCLUSIONS

We have used a combination of several scanning probe techniques to assess the influence of surface polarity and the presence of inversion domain boundaries on net Mg acceptor concentration in *p*-type GaN grown by MBE. Scanning capacitance microscopy and spectroscopy clearly reveal that, under identical growth conditions, net Mg acceptor incorporation occurs more effectively for Ga-face polarity than for N-face polarity. In addition, Ga-face material exhibits considerably better surface morphology than N-face material. However, only a minimal dependence of surface potential on polarity is observed in SKPM measurements—in contrast to observations of the dependence of Schottky barrier height on polarity for *n*-type GaN. SCM imaging also shows that elevated net concentrations of ionized Mg acceptors can be present in Ga-face regions, but not N-face regions, in the vicinity of inversion domain boundaries. This observation lends credence to recent theoretical work suggesting that increased concentrations of Mg acceptors could be present in the vicinity of inversion domain boundaries containing high concentrations of Mg within the domain boundary.

## ACKNOWLEDGMENTS

Part of this work was supported by the National Science Foundation (Award Nos. DMR 0072912 and DMR 0405851) and ONR (POLARIS MURI, Grant No. N00014-99-1-0729 monitored by Dr. Colin Wood).

[1]D. P. Bour, H. F. Chung, W. Goetz, L. T. Romano, B. S. Krusor, D. Hofstetter, S. Rudaz, C. P. Kuo, F. A. Ponce, N. M. Johnson, M. G. Craford, and R. D. Bringans, in *III-V Nitrides*, MRS Symposia Proceedings No. 449, edited by F. A. Ponce, T. D. Moustakas, I. Akasaki, and B. A. Monemar (Materials Research Society, Pittsburgh, 1997), p. 509.
[2]L. T. Romano, M. Kneissl, J. E. Northrup, C. G. Van de Walle, and D. W. Treat, Appl. Phys. Lett. **82**, 2278 (2003).
[3]P. Vennéguès, M. Benaissa, B. Beaumont, E. Feltin, P. De Mierry, S. Dalmasso, M. Leroux, and P. Gibart, Appl. Phys. Lett. **77**, 880 (2000).
[4]Z. Liliental-Weber, M. Benamara, W. Swider, J. Washbum, I. Grzegory, S. Porowski, D. J. H. Lambert, C. J. Eiting, and R. D. Dupuis, Appl. Phys. Lett. **75**, 4159 (2000).
[5]B. S. Simpkins, E. T. Yu, U. Chowdhury, M. M. Wong, T. G. Zhu, D. W. Yoo, and R. D. Dupuis, J. Appl. Phys. **95**, 6225 (2004).
[6]V. Ramachandran, R. M. Feenstra, W. L. Samey, L. Salamanca-Riba, J. E. Northrup, L. T. Romano, and D. W. Greve, Appl. Phys. Lett. **75**, 808 (1999).
[7]D. S. Green, E. Haus, F. Wu, L. Chen, U. K. Mishra, and J. S. Speck, J. Vac. Sci. Technol. B **21**, 1804 (2003).
[8]L. T. Romano, J. E. Northrup, A. J. Ptak, and T. H. Myers, Appl. Phys. Lett. **77**, 2479 (2000).
[9]J. E. Northrup, Appl. Phys. Lett. **82**, 2278 (2003).
[10]E. J. Tarsa, B. Heying, X. H. Wu, P. Fini, S. P. Den, and J. S. Speck, J. Appl. Phys. **82**, 11 (1997).
[11]M. Seelmann-Eggebert, J. L. Weyher, H. Obloh, H. Zimmermann, A. Rar, and S. Porowski, Appl. Phys. Lett. **71**, 2635 (1997).
[12]J. L. Rouviere, J. L. Weyher, M. Seelmann-Eggebert, and S. Porowski, Appl. Phys. Lett. **73**, 668 (1998).
[13]K. V. Smith, E. T. Yu, J. M. Redwing, and K. S. Boutros, Appl. Phys. Lett. **75**, 2250 (1999).
[14]D. M. Schaadt, E. J. Miller, E. T. Yu, and J. M. Redwing, Appl. Phys. Lett. **78**, 88 (2001).
[15]S. M. Sze, *Physics of Semiconductor Devices*, 2nd ed. (Wiley, New York, 1981).
[16]B. S. Simpkins, E. T. Yu, P. Waltereit, and J. S. Speck, J. Appl. Phys. **94**, 1448 (2003).
[17]B. S. Simpkins, E. T. Yu, U. Chowdhury, M. M. Wong, T. G. Zhu, D. W. Yoo, and R. D. Dupuis, J. Appl. Phys. **95**, 6225 (2004).
[18]U. Karrer, O. Ambacher, and M. Stutzmann, Appl. Phys. Lett. **77**, 2012 (2000).
[19]Z.-Q. Fang, D. C. Look, P. Visconti, D.-F. Wang, C.-Z. Lu, F. Yun, H. Morkoç, S. S. Park, and K. Y. Lee, Appl. Phys. Lett. **78**, 2178 (2001).
[20]D. M. Schaadt and E. T. Yu, J. Vac. Sci. Technol. B **20**, 1671 (2002).
[21]L. K. Li, M. J. Jurkovic, W. I. Wang, J. M. Van Hove, and P. P. Chow, Appl. Phys. Lett. **76**, 1740 (2000).